

Electronic Supporting Information

Nano-Affi: A Solution-Phase, Label-Free, Colorimetric Aptamer Affinity Assay Based on Binding-Inhibited Aggregation of Gold Nanoparticles

Yuan Wan,^a Jiaxing Zhao,^a Junlin He^b and Xinhui Lou ^{*a}

^a Department of Chemistry, Capital Normal University, Beijing, 100048, China

^b State Key Laboratory of Toxicology and Medical Countermeasures, Beijing Institute of Pharmacology and Toxicology, Beijing, 100850, China

* To whom correspondence should be addressed. Tel: +86-10-68902491 ext. 808; Fax: +86-10-68902320; Email: xinhuilou@cnu.edu.cn

Corresponding Author

* Email: xinhuilou@cnu.edu.cn

Tel: +86-10-68902491 ext. 808.

Fax: +86-10-68902320.

A Table of Contents

Chemicals and Materials	S-4
Supplementary Methods	S-4
Synthesis of 13 nm in diameter citrated-coated AuNPs	S-4
AuNP-lysozyme aggregates had high stability	S-5
Binding induced aggregation of gold nanoparticles assay	S-5
Dissociation kinetics measurements of lysozyme-aptamer complex using fluorescence waveguide sensor.....	S-5
Dissociation constant measurements using fluorescence waveguide sensors.....	S-6
Table S1	S-7
Table S2	S-7
Figure S1	S-8
Figure S2	S-8
Figure S3	S-9
Figure S4	S-9
Figure S5	S-10
Figure S6	S-10
Figure S7	S-11
Figure S8	S-11
Figure S9	S-12
Figure S10	S-12
Figure S11	S-13
Figure S12	S-13

Figure S13	S-14
Figure S14	S-14
Figure S15	S-15
Figure S16	S-15
Figure S17	S-16
Figure S18	S-16
Figure S19	S-17
Figure S20	S-18
Reference	S-19

Chemicals and Materials. All oligonucleotides (sequences shown in **ESI, Table S1**) were synthesized and purified by Sangon Biotech. (Shanghai, China). Lysozyme, thrombin, HSA, trisodium citrate salt dihydrate, sodium phosphate monobasic dihydrate ($\text{NaH}_2\text{PO}_4 \cdot 2\text{H}_2\text{O}$), and sodium phosphate dibasic dodecahydrate ($\text{Na}_2\text{HPO}_4 \cdot 12\text{H}_2\text{O}$) were purchased from Sangon Biotech. Gold (III) chloride trihydrate ($\text{HAuCl}_4 \cdot 3\text{H}_2\text{O}$) was purchased from J&K Scientific (Peking, China). Buffer solutions and 13-nm AuNP preparations were respectively filtered by 0.22 μm polyether sulphone and 0.22 μm cellulose acetate membranes (Sangon Biotech) immediately after being prepared, and then stored at 4 °C. Water purified by Millipore filtration was used for all experiments. The following binding buffer recipes were used for each protein target: lysozyme (20 mM Tris, 100 mM NaCl, 5 mM MgCl_2 , pH 7.4), thrombin (50 mM Tris, 100 mM NaCl, 1 mM MgCl_2 , 5 mM KCl, 1 mM CaCl_2 and 0.01% Tween 20, pH 7.5) ¹, and HSA (50 mM Tris, 100 mM NaCl, 1 mM MgCl_2 , 5 mM KCl, 1 mM CaCl_2 , pH 7.4) ².

Supplementary Methods

Synthesis of 13-nm diameter citrate-coated AuNPs. AuNPs were synthesized using a standard citrate reduction process ³. All glassware was cleaned in aqua regia ($\text{HCl}:\text{HNO}_3 = 3:1$), rinsed with Millipore water, and then oven-dried prior to synthesis. An aqueous solution of 200 mL 1 mM HAuCl_4 was heated and refluxed for 10 min while stirring. 20 mL of 38.8 mM trisodium citrate solution was quickly added, producing an immediate color change from pale yellow to wine red. After 15 min refluxing, the solution was slowly cooled to room temperature in a heating mantle and subsequently filtered through a 0.22- μm cellulose nitrate filter. The final AuNP concentration was 10.3 nM, based on UV-vis adsorption spectroscopy (extinction coefficient of $2.7 \times 10^8 \text{ M}^{-1}\text{cm}^{-1}$ at 520 nm), and the AuNP diameter was found to be 13 nm based on transmission electron microscopy measurement. The solution was stored at 4 °C.

AuNP-lysozyme aggregates had high stability. 50 μL of 80 nM lysozyme solution in 2X binding buffer was incubated with 50 μL of 10 nM AuNPs for 30 min at room temperature. Photos were taken and DLS measurements and UV-vis spectra were recorded. Then 1 μL of 8 μM Lyso48 or DNA44 in water was added to the AuNP/lysozyme mixture. The mixture was mixed well and rotated for 30 min at room temperature. Photos were taken and DLS measurements and UV-vis spectra were recorded. These results confirmed that neither DNA sequence could disassemble the

aggregates (**Figure S1**).

Binding-induced aggregation of AuNP assay. 2 μL of 8 μM non-binding sequence TBA15 or aptamer Lyso48 in water were incubated with 100 μL of 4 nM AuNPs for 30 min at room temperature. Photos were taken and DLS measurements and UV-vis spectra were recorded. We then added 100 μL of 80 nM lysozyme in 2X binding buffer to the AuNP/DNA mixture. After 30 min incubation at room temperature, photos were taken and DLS measurements and UV-vis spectra were recorded.

Dissociation kinetics of protein-aptamer complexes measured by a fluorescence waveguide sensor. The waveguide sensor employed in this study (all fiber optical system, single channel, Anheng Environmental Science and Technology, Ltd., Beijing, China) was prepared as described in Ref. ⁴. The fiber was immersed in piranha solution (3:1 [v/v] $\text{H}_2\text{SO}_4/\text{H}_2\text{O}_2$) at 120 $^\circ\text{C}$ for 60 min, and then rinsed with Milli-Q water. The cleaned fiber was dried with nitrogen flow and kept in an oven at 70 $^\circ\text{C}$ overnight. The fiber was then immersed in a 2% (v/v) 3-aminopropyltriethoxysilane (APTS) toluene solution for 60 min at room temperature, followed by thorough rinsing with absolute toluene, and then dried by nitrogen flow. The fibers were kept in an oven at 200 $^\circ\text{C}$ for 60 min. The fiber was then immersed in 2.5% (v/v) glutaraldehyde solution at 37 $^\circ\text{C}$ for 2 h to introduce aldehyde groups onto the fiber surface, and then washed thoroughly with Milli-Q water. The fiber was then immersed in 40 nM lysozyme or 2 mg/mL HSA in binding buffer at room temperature for 3 h to covalently couple protein onto the fiber. Finally, the fiber was incubated in 0.3 % NaBH_4 solution for 10 min at room temperature to reduce the imine bond to a stable C-N bond. The fibers were finally stored at 4 $^\circ\text{C}$ in a humid container prior to use.

The protein-coated fiber was then installed into the fiber chamber of the waveguide sensor. The pipe and chamber were rinsed with binding buffer at a flow rate of 30 $\mu\text{L}/\text{s}$ for 40 s. 40 nM Cy5.5-labeled aptamer Lyso48 or HSA50 solution was then pumped into the chamber at a flow rate of 15 $\mu\text{L}/\text{s}$ for 20 s to fill the chamber. The pump was then stopped, and the aptamer solution was retained in the chamber for 800 s to achieve binding equilibrium between aptamer and protein on the fiber. Next, the dissociation buffer (standard binding buffer or binding buffer diluted in 3.5 mM trisodium citrate solution at pH 6.5 or 4.9) was pumped into the chamber at a flow rate of 15 $\mu\text{L}/\text{s}$ for 20 s to replace the aptamer solution with dissociation buffer. The 3.5 mM trisodium citrate solutions used here were the same AuNP buffers used elsewhere in this study. The pump was then stopped, and the buffer was retained in the chamber for 800 s. The *in-situ* fluorescence responses,

including binding and dissociation of the Cy5.5-aptamer, were recorded by the sensor. The sensor was regenerated by pumping 0.5 M NaOH solution at a flow rate of 30 $\mu\text{L/s}$ for 60 s, followed by binding buffer at a flow rate of 30 $\mu\text{L/s}$ for 40 s.

Dissociation constant measurements using fluorescence waveguide sensors. The sensor was prepared as described above. After the NaBH_4 reduction step, the HSA-coated fiber was further blocked with 0.1% Tween 80 at room temperature for 30 min. Binding buffer was pumped into the chamber at a flow rate of 5 $\mu\text{L/s}$ for 30 s to achieve a stable baseline. Then, Cy5.5-labeled aptamer solutions of various concentrations in binding buffer were sequentially pumped into the chamber and incubated with the HSA-immobilized fiber at room temperature for 3 min. The fluorescence signal was recorded in real-time. After each measurement, the sensor was regenerated by pumping through 0.5 M NaOH at a flow rate of 15 $\mu\text{L/s}$ for 1 min and then binding buffer until reaching a stable baseline. The fluorescence intensity values 200 s after the injection of aptamer were plotted as a function of the concentration of aptamer. The dissociation constant was obtained by non-linear fitting assuming 1:1 binding.

Table S1. DNA sequences used in this study

Name	Sequence (5' to 3')	Description
DNA15	TGGATGATGTGGTAT	random sequence
DNA24	TAGCTATGGAATTCCTCGTAGGCA	random sequence
DNA29	ATTGACCGCTGTGTGACGCAACTCAAT	streptavidin aptamer ⁵
DNA30	GACAAGGAAAATCCTTCAATGAAGTGGGTC	cocaine aptamer ⁶
DNA44	ACGGGCCACATCAACTCATTGATAGACAATGCGTCCACTGCCCG	PD-L1 aptamer ⁷
DNA76	CGTACGGAATTCGCTAGCCCCCGCAGGCCACGGCTTGGGTTGGTCCCACTGCGCGTGGAT CCGAGCTCCACGTG	Tetracycline aptamer ⁸
Lyso48	CAGTGTATCTACGAATTCATCAGGGCTAAAGAGTGCAGAGTTACTTAG	lysozyme aptamer ⁹
TBA15	GGTTGGTGTGGTTGG	thrombin aptamer ¹⁰
TBA29	AGTCCGTGGTAGGGCAGGTTGGGGTGACT	thrombin aptamer ¹¹
HSA50	GTCTCAGCTACCTTACCGTATGTGGCCAAAGCGTCTGGATGGCTATGAA	HSA aptamer ¹²
HSA-6	GACAGACAGCCGAAATACGGACGAGACGAGCTTATGCGTAGCCTCTAGTGATTAAC GCAG	HSA aptamer ²
M1	GCCGAAATACGGACGAGACGAGCTTATGCGTAGCCTCTAGTGATTAACGCAG	Truncated HSA-6
M2	GCCGAAATACGGACGAGATGCGTAGCCTCTAGTGATTAACGCAG	Truncated HSA-6
M3	GCCGAAATACGGACTATGCGTAGCCTCTAGTGATTAACGCAG	Truncated HSA-6
M4	AGCTTATGCGTAGCCTCTAGTGATTAACGCAG	Truncated HSA-6
M5	GCCGAAATACGGACGAGACGAGCTTATGC	Truncated HSA-6
M6	AACGCAGGCCGAAATACGGACGAGACGAGCTTATGCGTA	Mutated HSA-6

Table S2. Comparison of frequently applied techniques for protein aptamer affinity evaluation

Method	Nano-Affi	ITC	EMSA	SPR	Affinity chromatography	ELONA
Labeling required	No	No	Yes	Yes	Yes	Yes
Immobilization required	No	No	No	Yes	Yes	Yes
Separation of bound and unbound aptamer	No	No	Yes	Yes	Yes	Yes
High throughput	Yes	No	Yes	Yes	Yes	Yes
Sample volume (μL)	10-50	200	10-20	200-500	100	100
Assay time	10-20 min	3-6 h	4-6 h	4-10 h	4-6 h	4-10 h
Training time	5 min	1 day	1 day	1 day	1 day	1 day
Sophisticated Instruments	No	Yes	No	Yes	No	No

EMSA: electrophoretic mobility shift assay

ELONA: enzyme-linked oligonucleotide assay

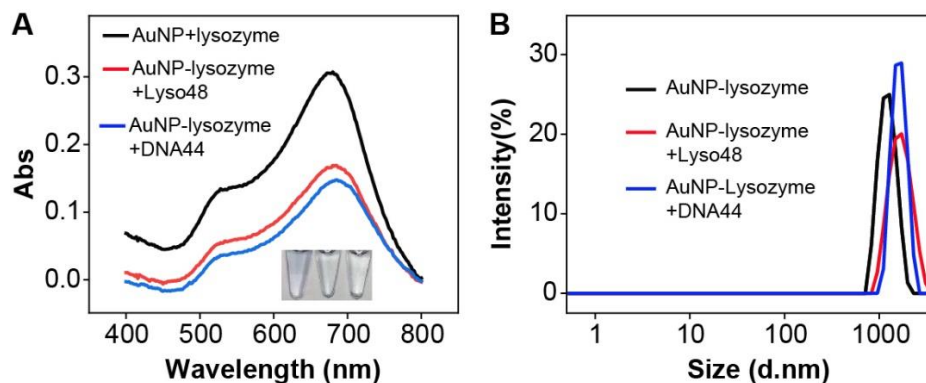


Figure S1. AuNP-lysozyme aggregates had high stability. **(A)** UV-vis absorption spectra and **(B)** hydrodynamic size of AuNPs 30 min after the addition of lysozyme alone (black) or with aptamer Lyso48 (red) or non-binding sequence DNA44 (blue). Inset in **A** shows photos of color change. Final concentrations of AuNP, Lyso48/DNA44, and lysozyme were 5, 80, and 40 nM, respectively.

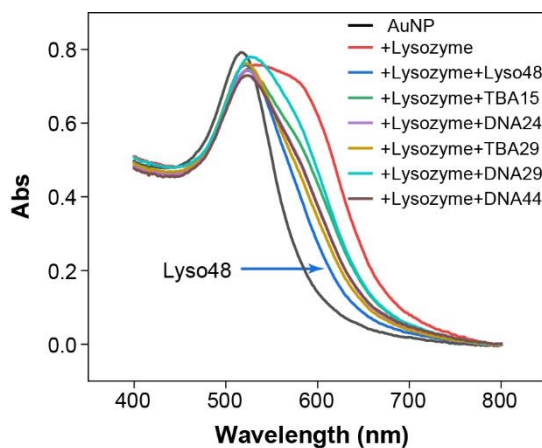


Figure S2. UV-vis absorption spectra recorded 10 min after the addition of 2 μ L lysozyme solution in binding buffer to 98 μ L of 2 nM AuNPs either alone or with Lyso48 aptamer or various non-binding sequences. The pH was 6.5, and final concentrations of lysozyme and DNAs were all 40 nM.

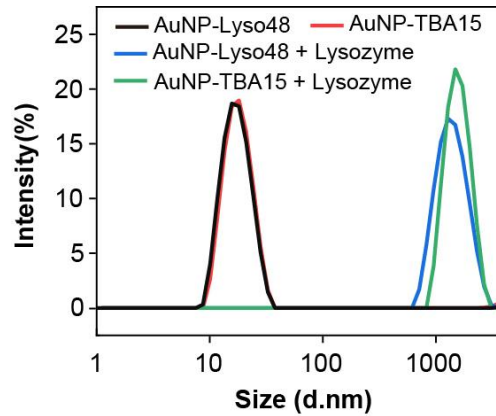


Figure S3. Binding-induced aggregation of AuNPs as a readout for lysozyme aptamer screening. Hydrodynamic size of AuNPs 30 min after the addition of aptamer Lyso48 or non-binding sequence TBA15 to an AuNP solution either alone (black and red) or with lysozyme (blue and green). Final concentrations of AuNPs, Lyso48/TBA15, and lysozyme were 2, 40, and 40 nM, respectively.

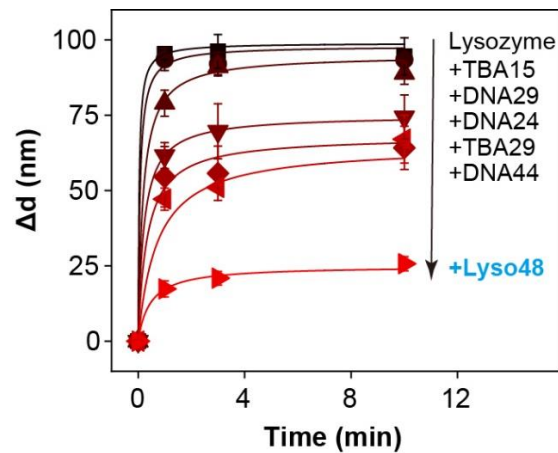


Figure S4. Kinetic Δd of AuNPs after addition of lysozyme alone or with aptamer Lyso48 or various non-binding sequences at pH 6.5. Each assay contained 40 nM lysozyme, 40 nM ssDNA and 2 nM AuNPs. Error bars show standard deviation of three repeat experiments.

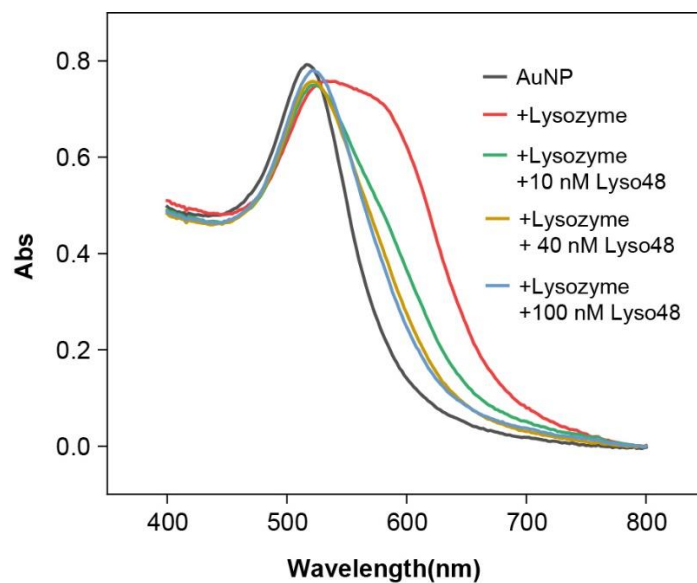


Figure S5. UV-vis absorption spectra 10 min after mixing lysozyme with AuNPs either alone or with various concentrations of aptamer. Each assay contained 40 nM lysozyme and 2 nM AuNPs at pH 6.5.

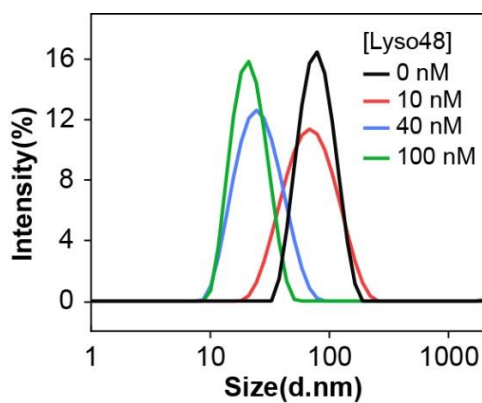


Figure S6. Hydrodynamic sizes of AuNPs 10 min after mixing with lysozyme alone or with aptamer Lyso48 at different concentrations. Each assay contained 40 nM lysozyme and 2 nM AuNPs at pH 6.5.

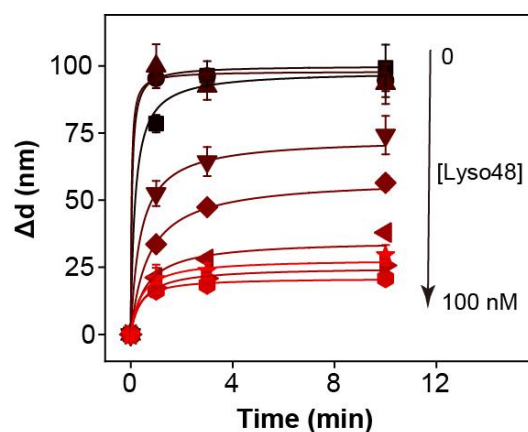


Figure S7. Kinetic Δd of AuNPs upon addition of lysozyme alone or with Lyso48 at different concentrations. Each assay contained 40 nM lysozyme and 2 nM AuNPs at pH 6.5. Error bars show standard deviation of three repeat experiments.

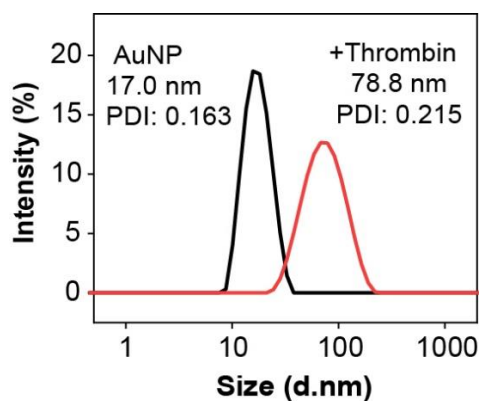


Figure S8. Hydrodynamic size of AuNPs after 10 min incubation with 40 nM thrombin at pH 6.5. The final concentration of AuNPs was 2 nM.

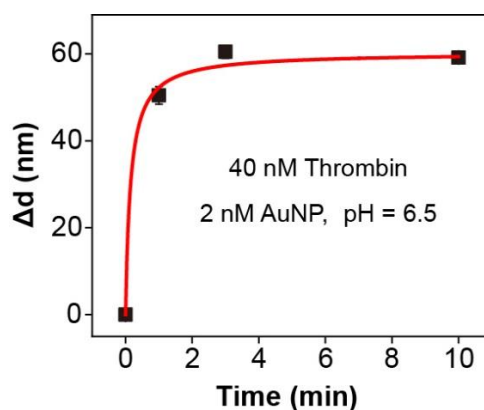


Figure S9. Kinetic Δd of AuNPs upon addition of thrombin. Error bars show standard deviation of three repeat experiments.

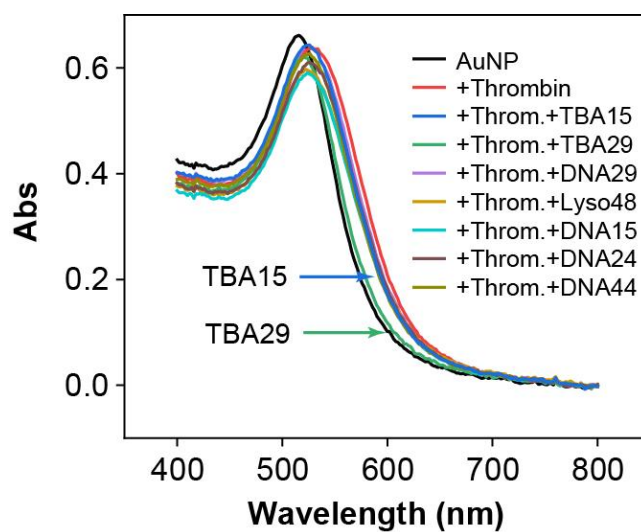


Figure S10. UV-vis absorption spectra recorded 10 min after adding 2 μ L of thrombin in binding buffer to 98 μ L of 2 nM AuNPs either alone or with aptamers or non-binding sequences at pH 6.5. The final concentration of thrombin and DNAs were all 40 nM.

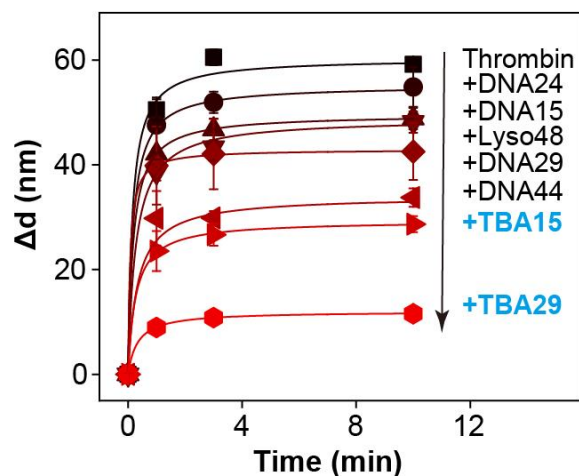


Figure S11. Kinetic Δd of AuNPs after addition of thrombin alone or with aptamers TBA15 or TBA29 or various non-binding sequences at pH 6.5. Each assay contained 40 nM thrombin, 40 nM DNA and 2 nM AuNPs. Error bars show standard deviation of three repeat experiments.

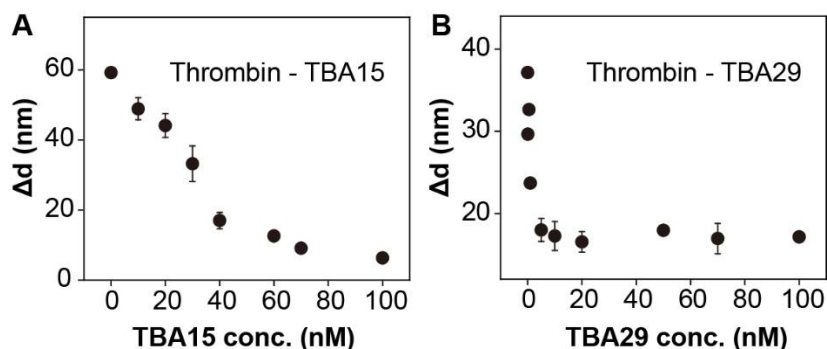


Figure S12. Nano-Affi for thrombin K_D determination. Δd of AuNPs 10 min after addition of thrombin alone or with aptamer TBA15 (A) or TBA29 (B) at a range of concentrations. All assays were performed at pH 6.5 with 2 nM AuNPs and a final concentration of thrombin was 40 and 2 nM for (A) and (B), respectively.

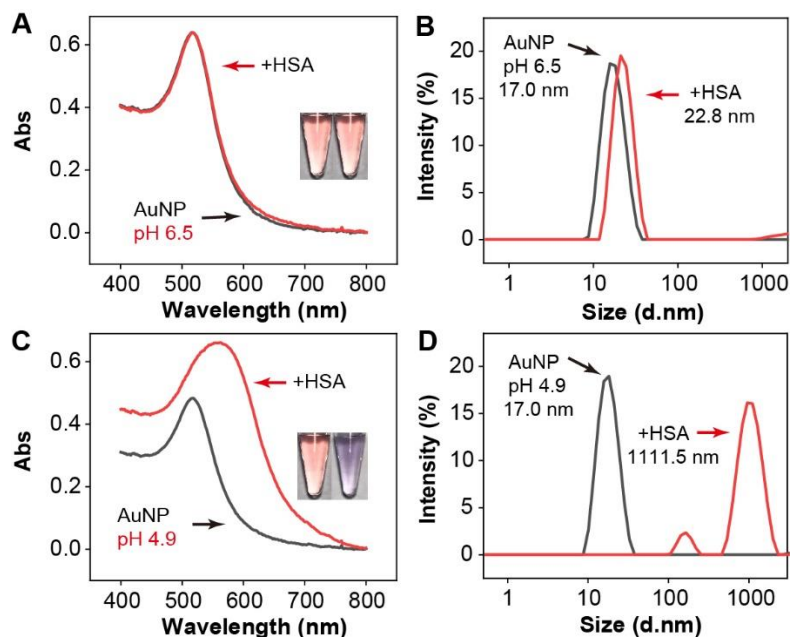


Figure S13. (A, C) UV-vis absorption spectra and (B, D) DLS measurements recorded 10 min after the addition of 2 μ L HSA in binding buffer to 98 μ L of 2 nM AuNPs at pH of 6.5 (A, B) or 4.9 (C, D). The final concentration of HSA was 40 nM.

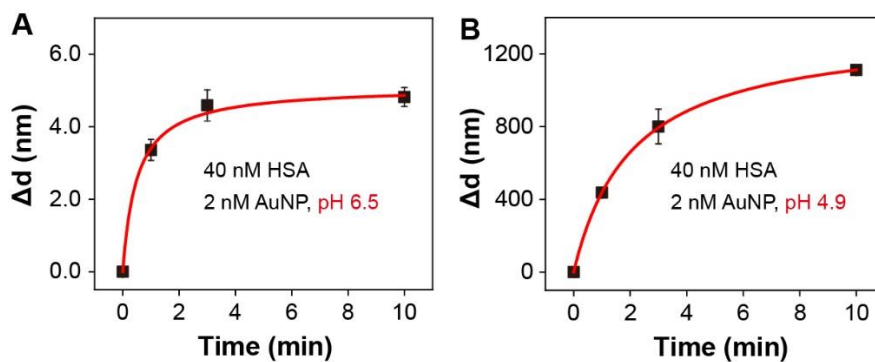


Figure S14. Kinetic Δd of AuNPs at pH 6.5 (A) and 4.9 (B) upon addition of HSA. Error bars show standard deviation of three repeat experiments.

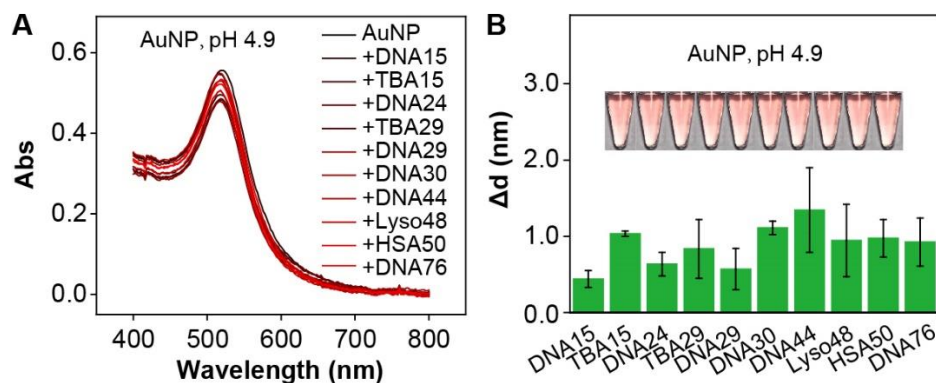


Figure S15. (A) UV-vis absorption spectra and (B) Δd of AuNPs at pH 4.9 10 min after the addition of various ssDNAs. Insets in B show photos of assay color. Error bars show standard deviation of three repeat experiments.

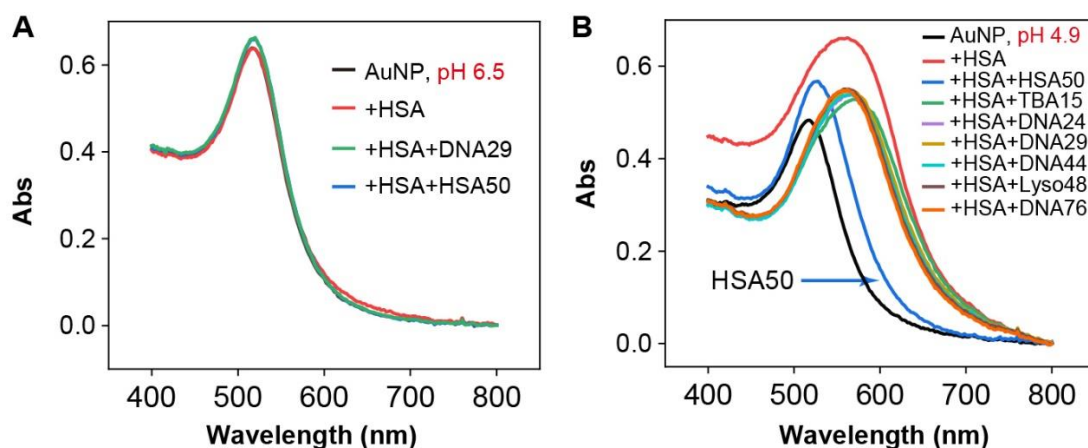


Figure S16. UV-vis absorption spectra recorded 10 min after addition of 2 μ L HSA in binding buffer to 98 μ L of 2 nM AuNPs, either alone or with aptamer HSA50 or various non-binding sequences at pH 6.5 (A) and 4.9 (B). Each assay contained 40 nM HSA and 40 nM ssDNA.

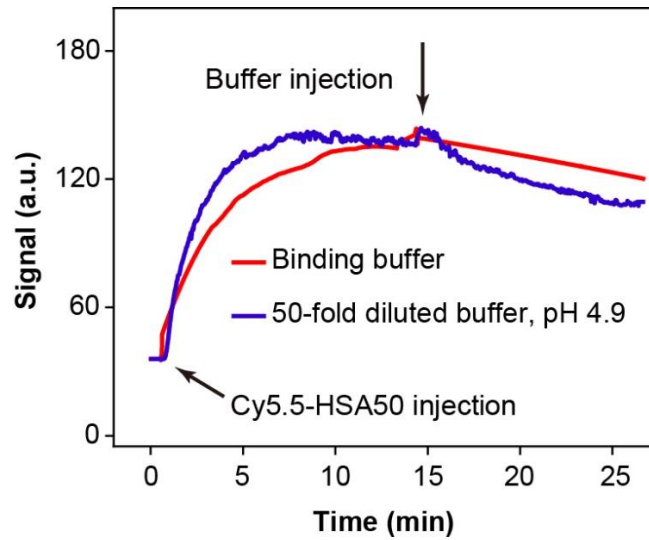


Figure S17. Binding and dissociation kinetics of HSA-HSA50 complexes in binding buffer or 50-fold diluted binding buffer at pH 4.9 as measured by fluorescence waveguide sensor. The optical fiber was immobilized with HSA and HSA50 was labelled with Cy5.5.

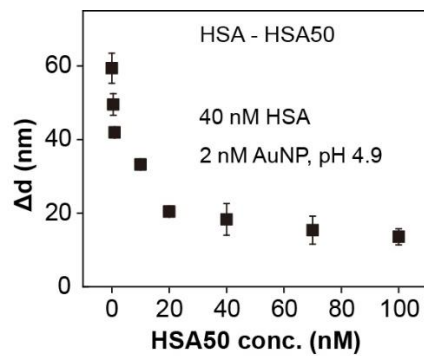


Figure S18. Nano-Affi for HSA K_D determination. Δd of AuNPs 10 min after the addition of thrombin alone or with aptamer various concentrations of aptamer HSA50.

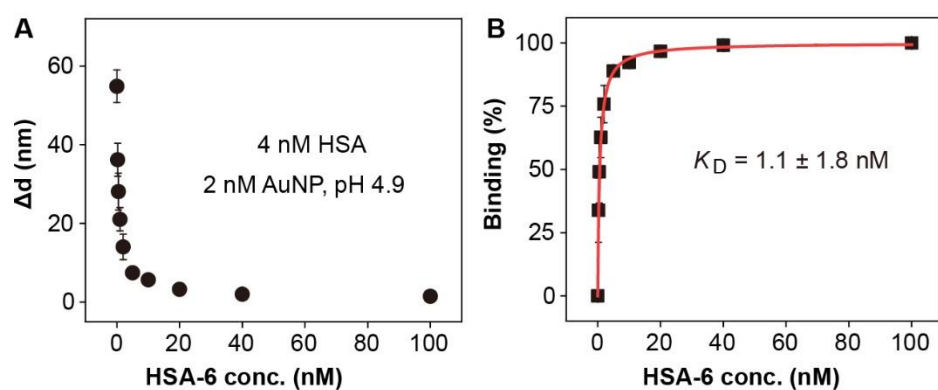


Figure S19. Dissociation constant determination of HSA-6 by Nano-Affi. **(A)** Hydrodynamic sizes of AuNPs in Nano-Affi assays in the presence of different concentrations of HSA-6. **(B)** The derived binding curve for K_D determination based on data shown in **A**. Error bars show standard deviation of three repeat experiments.

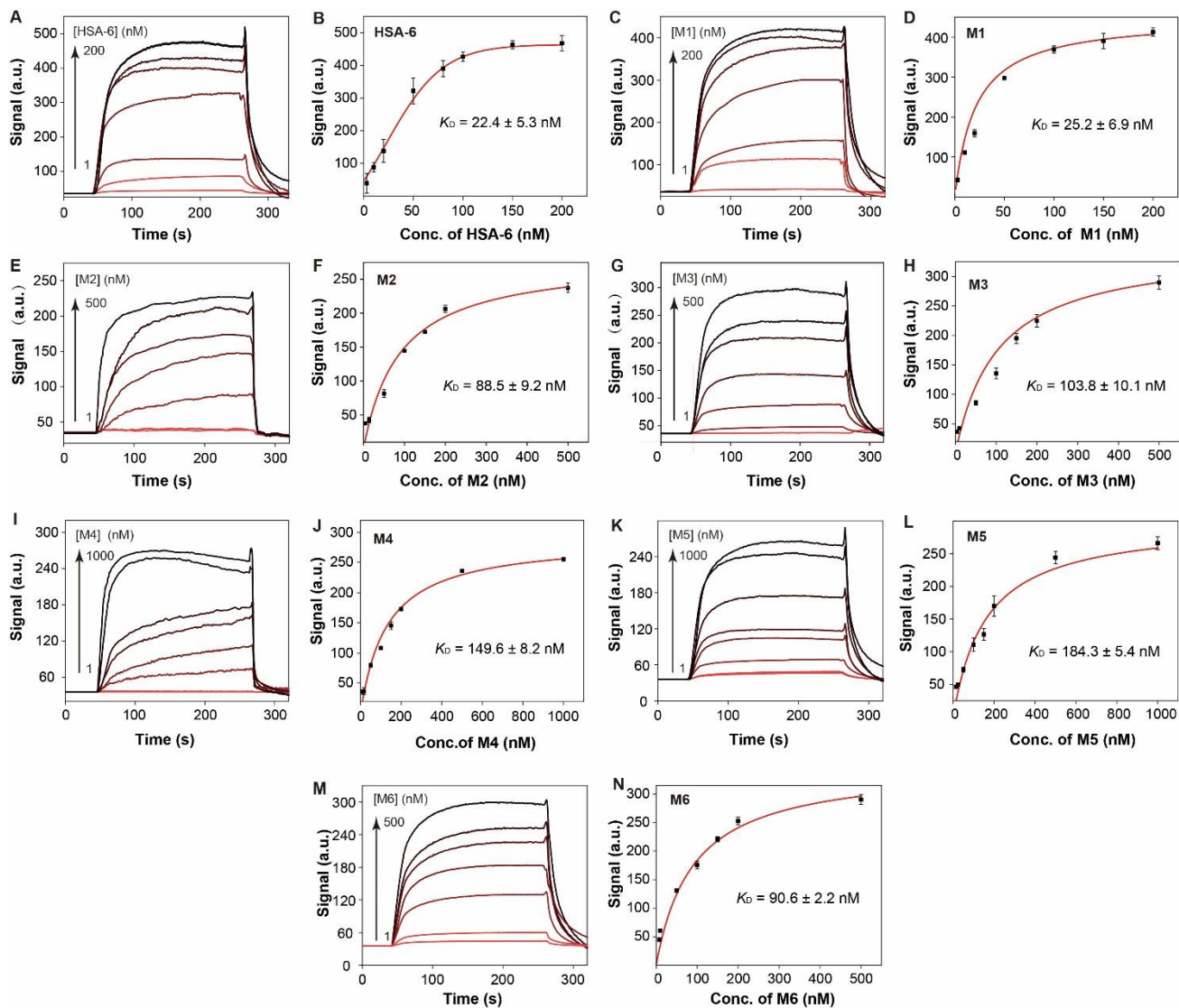


Figure S20. K_D determination of HSA-6 (A, B), M1 (C, D), M2 (E, F), M3 (G, H), M4 (I, J), M5 (K, L), and M6 (M, N) using waveguide sensors. A, C, E, G, I, K, and M show kinetic sensor responses upon injection of aptamers at different concentrations. B, D, F, H, J, L, and N are the derived binding curves for K_D determination based on fluorescence intensities 200 s after the injection of aptamer at different concentrations. Error bars show standard deviation of three repeat experiments.

Reference

1. K. M. Ahmad, Y. Xiao and H. T. Soh, *Nucleic Acids Res.*, 2012, **40**, 11777.
2. N. Qiao, J. Li, X. Wu, D. L. Diao, J. Zhao, J. Li, X. Ren, X. Ding, D. Shangguan and X. Lou, *Anal. Chem.*, 2019, **91**, 13383–13389.
3. G. Frens, *Nature Phys. Sci.*, 1973, **241**, 20; P. Ni, H. Dai, Y. Wang, Y. Sun, Y. Shi, J. Hu and Z. Li, *Biosens. Bioelectron.*, 2014, **60**, 286.
4. F. Long, M. He, H. C. Shi and A. N. Zhu, *Biosens. Bioelectron.*, 2008, **23**, 952.
5. T. Bing, X. Yang, H. Mei, Z. Cao and D. Shangguan, *Bioorg. Med. Chem.*, 2010, **18**, 1798.
6. M. N. Stojanovic, P. de Prada and D. W. Landry, *J. Am. Chem. Soc.*, 2001, **123**, 4928.
7. W. Lai, B. Huang, J. Wang, P. Lin and P. Yang, *Mol. Ther-Nucl. Acids* 2016, **5**, e397.
8. J. H. Niazi, S. J. Lee and M. B. Gu, *Bioorg. Med. Chem.*, 2008, **16**, 7245.
9. J. C. Cox and A. D. Ellington, *Bioorg. Med. Chem.*, 2001, **9**, 2525.
10. L. C. Bock, L. C. Griffin, J. A. Latham, E. H. Vermaas and J. J. Toole, *Nature*, 1992, **355**, 564.
11. D. M. Tasset, M. F. Kubik and W. Steiner, *J. Mol. Biol.*, 1997, **272**, 688.
12. M. Takenaka, Y. Okumura, T. Amino, Y. Miyachi, C. Ogino and A. Kondo, *Bioorg. Med. Chem. Lett.*, 2017, **27**, 954.